Exploring the Use of Temperature Transient Analysis During Pressure Falloff Testing in Geothermal Wells

Jorge Alberto Rangel Arista[1]*, Sadiq J. Zarrouk[1], Eylem Kaya[1], and Katie McLean[2]

[1] Department of Engineering Science, University of Auckland, Private Bag 90210, Auckland, New Zealand

[2] Contact Energy Ltd, Wairakei Power Station, Taupo, New Zealand

*jran489@aucklanduni.ac.nz

Keywords: *temperature transient analysis, pressure falloff testing, geothermal well.*

ABSTRACT

The transient temperature analysis could cast different information from geothermal formations. One technique that utilises transient temperature analysis is the static formation temperature test, a method that has several decades in use. On the other hand, a new technique called Temperature Transient Analysis (TTA) has been used in the last few years. This method uses the transient temperature data generated during pressure buildup or falloff tests to estimate certain parameters from geothermal reservoirs that could complement the analysis carried out using Pressure Transient Analysis (PTA). The present paper explores the possible outcomes that could be obtained using Temperature Transient Analysis (TTA) in conjunction with Pressure Transient Analysis (PTA).

1. INTRODUCTION

The Pressure Transient Analysis (PTA) has been used for several decades to determine parameters of the formation from the pressure and flow rate data. There are analytical and numerical PTA methods. The analytical techniques used simplifications to represent the phenomena. On the other hand, the numerical methods avoid simplifications; consequently, they could model the formation under the pressure test in a more realistic way. PTA is based on solving the pressure diffusion equation (1).

$$\frac{\partial P}{\partial t} = D_p\left(\frac{\partial^2 P}{\partial r^2} + \frac{1}{r}\frac{\partial P}{\partial r}\right) \tag{1}$$

where P is pressure (bar), r the well radius (m), t the time (s), D_p hydraulic diffusivity (m^2/s) equals to $k/(\phi\mu c_t)$, k the reservoir permeability (m^2), ϕ the reservoir porosity (dimensionless), μ dynamic viscosity of fluid (Pa·s), and c_t the total system (reservoir fluid and rock) compressibility (1/Pa).

The temperature data generated in single-well tests have often been neglected because most analytical solutions to equation (1) assume isothermal conditions. However, with the growing applications of numerical well-test analysis techniques (McLean and Zarrouk, 2017). This encouraged some authors to examine transient temperature because it provides reliable data to complement reservoir characterisation (Onur & Palabiyik, 2015). These studies opened the door to a new field to investigate transient temperature: Temperature Transient Analysis (TTA).

TTA is intended to analyse the transient temperature from drawdown/buildup and injection/falloff tests and its effects on nonisothermal models. This casts another perspective on the reservoir parameters. Usually, these variables have been studied by applying PTA; however, sometimes, this tool produces unconvincing results due to the lack of nonisothermal effects (Benson & Bodvarsson, 1986). Therefore, TTA complements PTA (Palabiyik et al., 2016; Ramazanov et al., 2010).

Although TTA studies are relatively recent, the basis was established several decades ago. In this sense, Carslaw & Jaeger (1959) developed the thermal diffusion equation (2), the primary expression for analysing transient temperature, which only represents thermal conduction (no convection). Another significant work was produced by Ramey (1962), who investigated the injection of fluids into boreholes and the heat transfer processes. This research was the first to attain an expression of temperature in terms of time and depth (Silva Junior et al., 2012). These two authors are the cornerstone to interpreting the transient temperature data, similarly to Horner (1951) for analysing transient pressure data.

$$\frac{\partial T}{\partial t} = D_t\left(\frac{\partial^2 T}{\partial r^2} + \frac{1}{r}\frac{\partial T}{\partial r}\right) \tag{2}$$

where T is temperature ($°C$). D_t the reservoir rock thermal diffusivity (m^2/s) equals to $\kappa/(\rho C_p)$, κ the overall (fluid and rock) thermal conductivity of porous media (W/m·K), and ρC_p the overall (fluid and rock) thermal capacity of porous media or the reservoir (J/K·m^3).

Besides the above, different researchers have investigated TTA to attain extra information from formations (Dada et al., 2017; Mao & Zeidouni, 2017). Others have studied the use of TTA in conjunction with PTA, such as Onur et al. (2008). They developed mass and energy balances to obtain expressions of the geothermal reservoir for pressure and temperature. Onur et al. (2008) concluded that utilising temperature and pressure matching may help estimate the bulk volume of the reservoir, porosity at initial temperature and pressure, and compressibility of porosity at a constant temperature.

Onur et al. (2016) worked with PTA expressions and the TTA analytical equations presented by Palabiyik et al. (2016). Then introduced, the temperature derivative concept (Equation 3) to identify all the lapses in the flow regime. Additionally, a methodology is proposed to analyse transient temperature/pressure data from drawdown/buildup tests. Onur et al. (2016) concluded that this methodology is able to compute the mobility of skin/non-skin zones, porosity, JT fluid coefficient, and skin zone radius using TTA and PTA.

ISSN 2703-4275

$$abs\left(T'_{\ln \Delta t}\right) = \left|\frac{dT}{d\ln \Delta t}\right| \quad (3)$$

Panini & Onur (2018) suggested an analytical model composed of PTA and TTA to estimate drawdown temperature/pressure transient behaviour for a vertical oil well in a radial composite reservoir. Panini & Onur (2018) concluded that using both TTA and PTA, it is possible to estimate near-wellbore properties accurately.

This paper presents the possible outcomes that could be obtained using the TTA in conjunction with PTA utilising numerical modelling when falloff data from a geothermal reservoir is analysed.

2. CASE OF STUDY

Data from well BR49 in the Ohaaki geothermal system, New Zealand, was selected as a case study. This well is in the east part of the geothermal system. It has a high-temperature feed zone of around 290°C with a total depth of 2798.20 m.

BR49 was stimulated using deflagration to enhance the near well permeability. After deflagration, an injection-falloff test was conducted. Figure 1 shows the injection period before the falloff. Multiple time steps could be seen; the last three steps before the falloff are 10.33, 15.66, and 19.83 kg/s. Then drop to 10.83 kg/s remaining at this value during the falloff. The falloff duration is about 28,980.00 seconds.

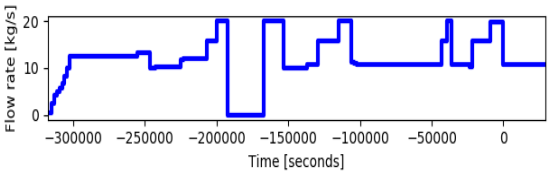

Figure 1: History of injection time steps before falloff.

Figure 2 shows the pressure, temperature, and flow rate during the falloff. The pressure drops in the first seconds keeping this moderate trend until it levels off momentarily. Then a gradual increase occurs during the remaining transient period. For temperature, a rapid rise occurs in the beginning, but suddenly the trend changes, maintaining the rising, but with a lower rate. The temperature reaches an equilibrium that continues in the remaining falloff.

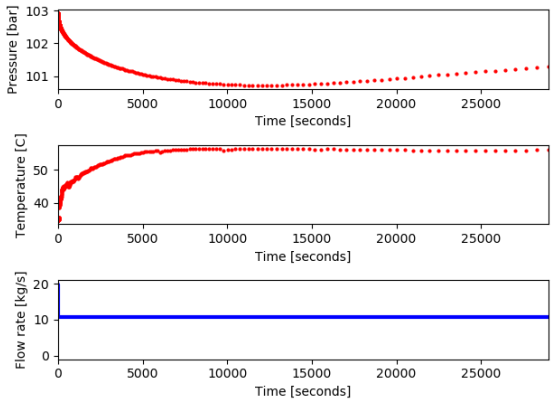

Figure 2: Pressure, temperature, and flow rate during the falloff.

3. MODEL SETUP

The TOUGH3 reservoir simulator was employed. This software is based on TOUGH2 (Pruess, 2012), a general-purpose simulator used to simulate geothermal reservoirs, which can model subsurface fluid and heat flow.

In the same way, PyTOUGH was employed to manage TOUGH3. PyTOUGH is a conjunction of scripts based on PYTHON to make it easier to use TOUGH3. This tool facilitates controlling all the aspects of TOUGH 3: grid construction, data files, analysis of results, etc. (Croucher, 2020).

The framework developed by Mclean & Zarrouk (2017) for the numerical modelling was used with a slight variation. Initially, this framework was created for the PTA of geothermal reservoir formations. Figure 3 shows the model grid structure Mclean & Zarrouk (2017) proposed, consisting of one cylindrical layer composed of multiple blocks spaced logarithmically. In the centre, it can be appreciated that one block represents the well. Then comes the skin zone ranging from 0 to 100 m approximately. Next to the skin area, the reservoir zone extends to a considerable distance from the well (20,000.00 m).

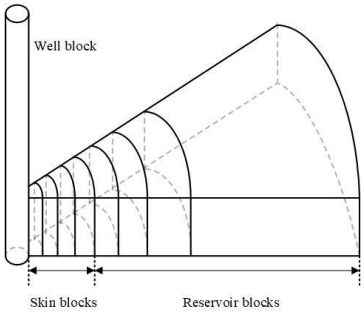

Figure 3: Model grid structure proposed by Mclean & Zarrouk (2017).

A variation of the Mclean & Zarrouk (2017) model was utilised for the present case. The variation consisted of employing three layers instead of one (Figure 4). Our modelling experiments showed that the inclusion of vertical dimension could be more representative of simulating temperature changes than just one layer. It follows the same areal grid structure as for one layer. Table 1 depicts the parameters used for the multiple-layer model. Several values were obtained from the actual well, such as well radius, payzone, etc.

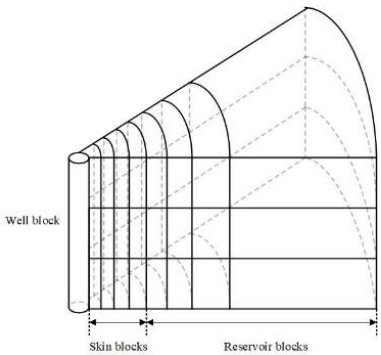

Figure 4: Grid structure of the present model.

Table 1: Multiple layer model parameters.

Maximum numerical timestep (s)	100
Equation of State (EOS)	EOS1
Well volume (m^3)	118.8
Reservoir thickness (m)	1080.0
Well radius (m)	0.10795
Well permeability: order of magnitude greater than reservoir permeability k	3
Model radial extent (km)	20
Number of layers	3

In conjunction with the Mclean & Zarrouk (2017) framework, the fractional dimension model was utilised to represent a fractured reservoir. This method represents better complex fractured reservoirs than others (Zarrouk et al., 2007). This concept surged from Barker (1988) generalised radial flow (GRF) model.

The fractional dimension model can take a number between one, two, and three. The number one represents a horizontal flow approximated as a slot or flowing along a plane. The number two depicts a horizontal flow that forms a flat round disk that converges in the well. And the number three is to emulate flow from all directions, creating a sphere converging in the well.

In order to represent the fractional dimension (n), it is necessary to modify the volume of the blocks as well as the contact area between them. Table 2 shows the required equations to modify the volume blocks and connection areas according to the number of fractions needed (O'Sullivan et al., 2005).

Table 2: Equations to compute block volumes and connection areas using the fractional dimension model.

Dimension of model	Block volumes	Connection areas
1	$2b^2\left(r_{i+1/2}-r_{i-1/2}\right)$	$2b^2$
2	$\pi b\left(r_{i+1/2}^2-r_{i-1/2}^2\right)$	$2\pi b r_{i+1/2}$
3	$(4\pi/3)\left(r_{i+1/2}^3-r_{i-1/2}^3\right)$	$4\pi r_{i+1/2}^2$
n	$\left(\alpha_n b^{3-n}/n\right)\left(r_{i+1/2}^n-r_{i-1/2}^n\right)$	$\alpha_n b^{3-n} r_{i+1/2}^{n-1}$

r: distance from the well; b: "thickness" of the fracture network; n: dimension of model; $\alpha_n = 2\pi^{n/2}/\Gamma(n/2)$, Γ: gamma function.

It is worth noting that the well/skin/reservoir systems are pretty complex during falloff to be fully represented even in numerical modelling. Thus, it is required to consider some simplifications in order to represent the model. In this regard, we took into account the existing similarities between the pressure diffusion (Equation 1) and temperature diffusion (Equation 2) expressions to model the temperature data. Under this consideration, it is much simpler to represent the heat transfer phenomenon because all the heat is transferred by "conduction", which in reality is a complex process formed by conduction, convection and radiation in conjunction with fluid flow in a porous media. Therefore, in this first attempt, this consideration was used to try to obtain more information from the reservoir. The subsequent works are expected to improve the model with more considerations as the number of wells analysed increases and cast more information about the geothermal formation.

3. RESULTS

For the numerical modelling, the falloff time was divided into multiple steps to reach the best match for the pressure and temperature data.

Usually, to attain the pressure match, the fractional dimension parameter changes over the steps while the other parameters remain constant. In this study, it was looked for pressure and temperature match at the same time. In this regard, the conventional parameters (reservoir permeability, skin factor, initial reservoir pressure, number of skin and reservoir blocks, layer thickness, skin zone radius, well radius, well volume, well porosity, well compressibility, well permeability, maximum timestep, model radial extent, injectate temperature, etc.) were used with fractional dimension for matching pressure and temperature. However, this procedure was inadequate to compute a suitable match for temperature. It is worth noting that these parameters change the model temperature in a limited range, which is not optimal for attaining a proper match. Thus, other variables that were more associated with thermal "conduction" were explored. The properties were thermal conductivity, density, and specific heat, representing the thermal diffusion coefficient (Equation 2). Changing the value of these parameters in every single step was sufficient to achieve a better fit for temperature data.

During the matching process, temperature changes have more influence on pressure rather than the other way around. For this reason, it is more convenient to start with the temperature data match by changing the thermal properties for the corresponding step.

Specific heat and thermal conduction are the thermal properties that have a significant influence on the temperature model. Once the temperature is matched in the corresponding step, the fractional dimension comes out for the pressure model. The fractional dimension variations unaffected the temperature model path. It just alters the heat transfer rate because reservoir and skin geometries are modified by this number and, consequently, the speed at which the heat transfer occurs.

The pressure and temperature have a thermodynamic-dependent relationship affecting the match in the first step on a large scale. The pressure is sensitive to several factors described by Mclean & Zarrouk (2017). However, for temperature, additional parameters must be considered. Thus, this task acquires more complexity because changes in every parameter modify pressure and temperature similarly. It becomes an iterative work to fit the best approximation. The complexity increases when it is considered the pressure derivative as well. Minimum changes create different modifications in the three responses (pressure, temperature, and pressure derivative).

Two models were considered. The first model takes into account just the pressure and temperature matches. The

second model includes pressure, temperature, and pressure derivative matches.

Table 3 shows the thermal properties of the well and skin zone. The well zone is considered single-phase liquid water at 290°C, which is the temperature feed zone. The thermal properties in the well zone were calculated utilising the equations provided by the International Association for the Properties of Water and Steam (IAPWS, 1996; IAPWS, 2008). For the skin zone, the values were taken from the work of Somerton (1992).

Table 3: Thermal properties values assigned for the well and skin zones.

	Thermal conductivity (W/m·K)	Density (kg/m^3)	Specific heat (J/kg·K)
Well zone	1.00	900.00	4500.00
Skin zone	3.00	2500.00	900.00

As mentioned above, we first matched the temperature data for the first case considered. Figure 5 depicts the thermal conductivity and specific heat changes along the falloff time. In the first moments, the thermal conductivity for both well and skin areas is relatively high, indicating that the primary heat transfer mechanism is convection, although we are only considering "conduction" for the model. This provokes the initial spike in the rising temperature. The thermal conductivity values decreased slightly in the following seconds, but the temperature increase remained. Regarding specific heat, the values were not significant at the beginning, but after the first seconds, rapid growth occurred. After the substantial increase in temperature passed, the thermal conduction started to decline, and the primary heat transfer mechanism changed from convection to conduction, whereas specific heat increased.

It can be observed that thermal conductivity and specific heat follow opposite tendencies as time passes by. Thermal conductivity decreases as the steps continue till the point where a change in this property is irrelevant. This change occurs when the temperature curve starts to flat, in which the specific heat has more influence over the temperature. In the end, the specific heat increases its value considerably, contrary to thermal conductivity. Despite this influence, obtaining a perfect match for the temperature at a late time was not achieved.

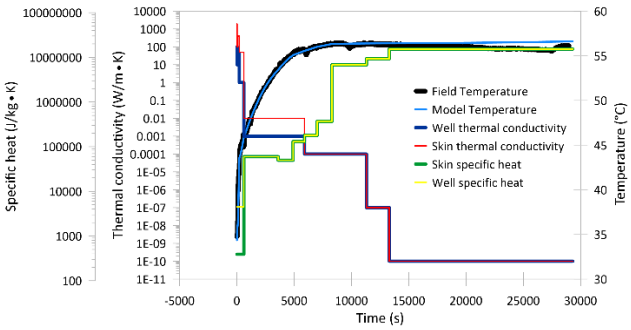

Figure 5: Thermal conductivity and specific heat changes along the falloff time, first case.

Figure 6 depicts the thermal diffusion coefficient for the well and skin zone during the falloff. Two kinds of thermal diffusion coefficients are displayed. The first one (real) is calculated using the values shown in Table 3 for the well and skin zone. The second one corresponds to the values (thermal conduction and specific heat) that change in every step along the falloff for the well and skin zone. These changing values are unrealistic but help us simplify the model and the complex inflow and wellbore convection in the geothermal well. For instance, using this approach, it could be appreciated that the heat transfer begins with significantly high values of thermal diffusion, which indicates that convection is probably the primary mechanism of heat transfer in these early times because "conduction" can not present these high values. Then these values start to decline along the falloff. In the end, considerable low values are seen, indicating that the primary heat transfer in these moments is conduction.

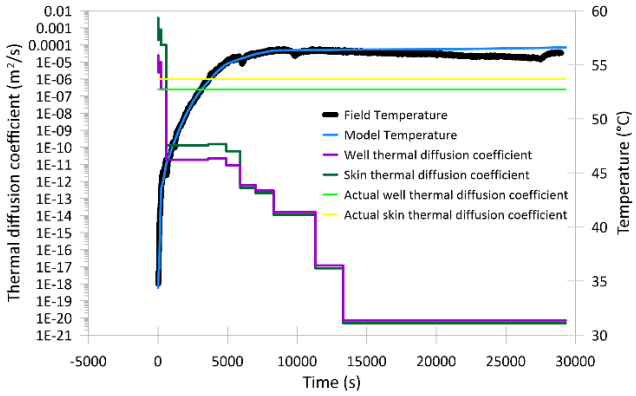

Figure 6: Thermal diffusion coefficient along the falloff time, first case.

Figure 7 shows the pressure and temperature match as well as the changing fractional dimension to attain a representative model. At the early time, it is observed that the formation is more predisposed to simulate a flow approaching the well radially from all directions. At this moment, pressure suffers a drop and temperature a rapid increase. Then the fractional dimension goes through an immediate change in which the flow approaches the well along a plane. The pressure and temperature maintained the same tendency but at a lower rate. Moments later, the fractional dimension started to increase and reached a value above 1.5. The pressure and temperature follow the same path with a decreased rate. Next, the fractional dimension varies around 1.7 the remaining time without significant changes. This behaviour implies that the formation is more inclined to emulate a disc. For the late time, the model temperature presented a slight fluctuation that diverged from the data. On the other hand, the pressure match in the late time is more accurate, but some fluctuations are presented.

Once the pressure and temperature were matched, we proceeded with the computation of the pressure derivative. Figure 8 depicts delta pressure (difference between shut-in and initial pressure) and pressure derivative. For delta pressure, the match at the beginning is not perfect, but after this period, the patterns align themselves better. On the other hand, the pressure derivative depicts fluctuations along the data at the beginning and middle. In the end, the match is better.

ISSN2703-4275

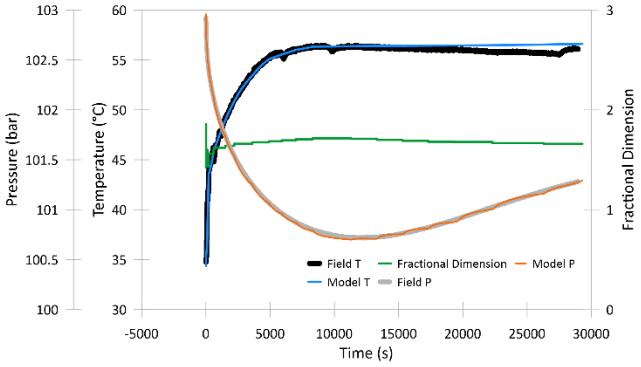

Figure 7: Fractional dimension corresponding to pressure and temperature match, first case.

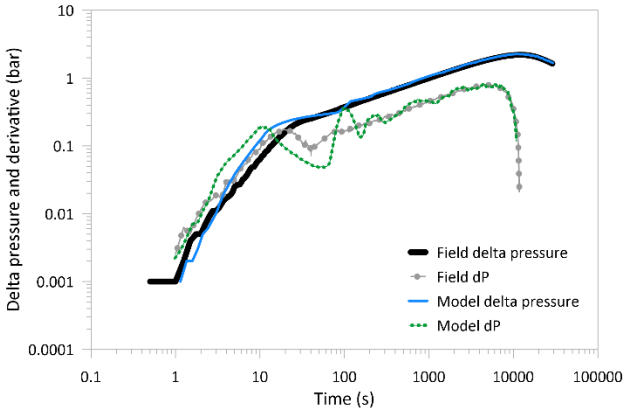

Figure 8: Delta pressure and pressure derivative, first case.

The temperature derivatives were calculated in the same way. For the calculations, Equation 2 was utilised. Figure 9 illustrates the delta and derivative temperature. For delta temperature (difference between shut-in temperature and initial temperature), there is not a good match following the data trend at the early and middle times. However, after ~ 200 seconds, the match is ideal without significant changes till the end. For the temperature derivative, the data shows several fluctuations which are not totally matched the model. Just some parts depict a suitable match.

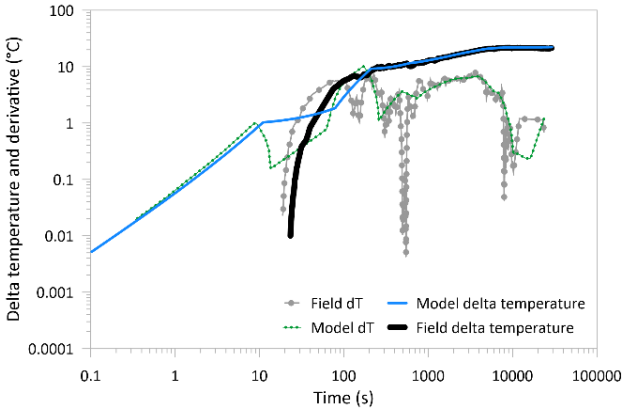

Figure 9: Delta temperature and temperature derivative, first case.

In the second model, the pressure, temperature, and pressure derivative were matched at the same time. In this regard, a similar procedure was followed, but additionally, pressure derivative was considered. Figure 10 depicts specific heat and conductivity. Both properties follow the same pattern as the first model in the first moments. Then a significant variation is observed; i.e., conductivity remains constant, whereas specific heat decreases momentarily at each step, then suffers a gradual rise. In the late time, both reach stabilisation values suddenly and stay at this value until the end. The first case depicted a couple of steps to achieve the final value, contrary to this case.

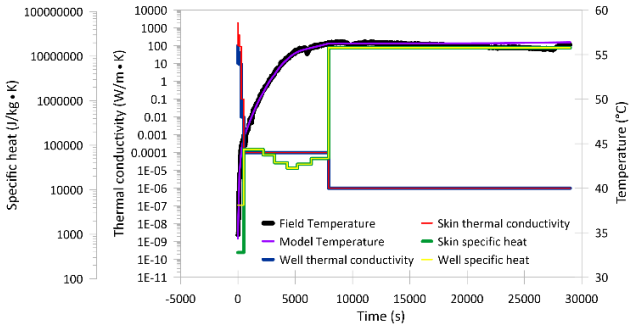

Figure 10: Thermal conductivity and specific heat changes along the falloff time, second case.

Similar to the first model, Figure 11 illustrates the thermal diffusion coefficient for the well and skin zone during the falloff. One of the main differences is that around 5000 s, the thermal diffusion coefficients appear to follow an increasing tendency but suddenly drop their values again. The other difference is associated with a faster stabilisation of the coefficients, reaching around 7500 s compared with the first case.

Figure 12 depicts the fractional dimension changes over the falloff to attain the respective matches. In the beginning, the fluid flow is just slightly declined to flow radially from all directions and converge in the well. Still, suddenly, it changes to flow along a plane and then increases to a value above 1.6, stabilising. During these first changes, pressure suffers a sharp decline, and temperature rapidly increases. Then the fractional dimension changes slightly around 1.7 during the remaining time. The most significant changes are at the early time compared with the first case. The pressure match has fewer fluctuations than in the previous case. Regarding temperature, the match is better than the first case, even though there is a slight variation between the data and the model in the late period.

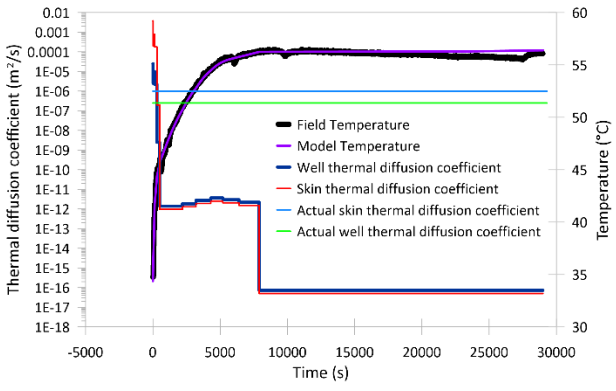

Figure 11: Thermal diffusion coefficient along the falloff time, second case.

ISSN2703-4275

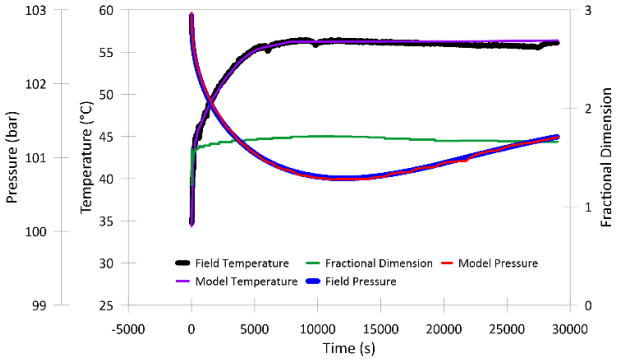

Figure 12: Fractional dimension corresponding to pressure and temperature match, second case.

Figure 13 illustrates the resulting delta pressure and pressure derivative. The match turns out better in this case. The model follows the trend depicted by the data.

After obtaining the above results, the delta temperature and temperature derivative were computed. Figure 14 shows that delta temperature is not matched just at the early time. This trend changes in the remaining time, when the match is suitable. For the temperature derivative, the data presents several fluctuations due to the nature of temperature. At the same time, the model does not precisely follow the data path but instead follows the general trend without all the instant changes.

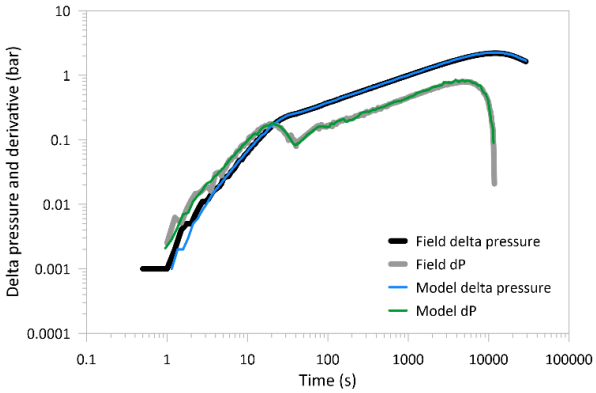

Figure 13: Delta pressure and pressure derivative, second case.

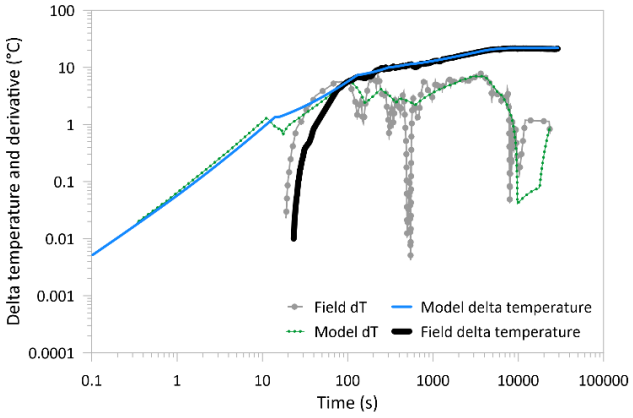

Figure 14: Delta temperature and temperature derivative, second case.

Figure 15 depicts the pressure and temperature derivative of the model. It appears that the temperature is more sensitive to the changes. Temperature follows the general path of pressure. The peaks and valleys are more considerable in temperature.

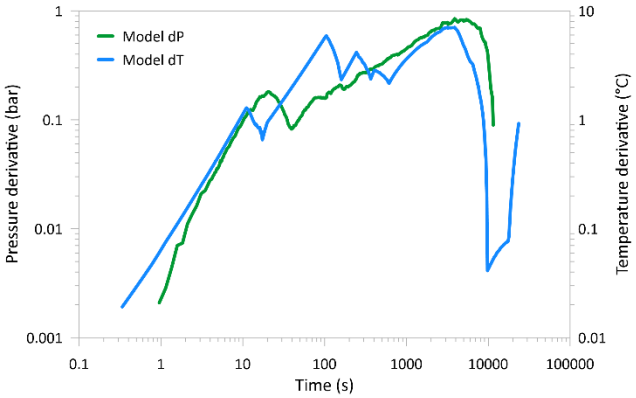

Figure 15: Pressure derivative and temperature derivative of the model, second case.

Finally, Table 4 compares different parameters when temperature data is considered. The estimated parameters depict a slight difference that is probably associated with the nonisothermal effects.

Table 4: Initial thermal properties values.

Parameters	Pressure and Temperature match	Pressure match
Injectate temperature (°C)	22.40	24.50
Reservoir permeability: k x10^{-15} m^2	29.1	30
Skin factor: s	-1.46	-1.5
Skin zone permeability: k_s x10^{-15} m^2	45.20	41
Number blocks in skin zone	40	40
Number blocks in the reservoir zone	60	60
Layer thickness h (m)	1080	1080
Skin zone radius r_s (m)	6.5	5.0
Well radius r_w	0.10795	0.10795
Well volume (m^3): vol. fluid in wellbore/0.9	126.66	126.66
Well porosity θ	0.9	0.9
Well permeability: order of magnitude greater than reservoir permeability k	3	3

Parameters	Pressure and Temperature match	Pressure match
Maximum timestep (s)	100	100
Model radial extent (km)	20	20
Number of layers	3	3

4. CONCLUSIONS

While wellbore temperature changes during pressure falloff tests are mostly related to the convective flow of hot reservoir fluid into the wellbore. The incorporation of temperature data in addition to pressure measurements for reservoir characterisation has shown that temperature measurements contribute to a better interpretation of well tests. In this study, we created a numerical framework to identify the reservoir characteristics of the transitional behaviour that produces pressure and temperature response. The method presented in this paper considers pressure, temperature, and their derivatives for sand, analysing this response during a falloff test. Our work shows that the derivative approach improves the analysis's interpretation and helps match field data better. This study also indicates that the variation of thermal conductivity and specific heat capacity (thermal diffusivity) under dynamic conditions enables a better temperature response than considering these thermal properties constant in conventional reservoir characterisation.

The drop in thermal diffusivity during pressure falloff means that the well mainly absorbs the heat, and only a small amount of heat is conducted through. This may change later, which could also help better understand the near well formation, the nature of permeability and the types of loss zones. Analysing more well-test data will help shed light on the applications of this method. In the same way, a sensitivity analysis will be conducted to obtain more information about the benefits of using this PTA-TTA framework.

ACKNOWLEDGEMENTS

The first author thanks the National Council of Science and Technology of Mexico (CONACYT) for kindly providing the PhD scholarship.

REFERENCES

Al-Nahdi, A., Gill, H.S., Kumar, V., Sid, I., Karunakaran, P., Azem, W.: Innovative Positioning of Downhole Pressure Gauges Close to Perforations in HPHT Slim Well During a Drillstem Test. *Proc. Offshore Technology Conference 2014*, Texas, USA. (2014).

Barker, J.A.: A sgeneralised radial flow model for hydraulic tests in fractured rock. *Journal of Water Resources Research*. pp. 1796–1804. (1988).

Benson, S.M., Bodvarsson, G.S.: Nonisothermal Effects During Injection and Falloff Tests. *Journal of SPE (Society of Petroleum Engineers) Format. Eval. 1986*, USA. pp. 53-63. (1986).

Carslaw, H.S., Jaeger, J.C.: Conduction of Heat in Solids. Oxford University Press, Great Britan, 1959.

Croucher, A.: PyTOUGH user's guide. Department of Engineering Science, University of Auckland. (2020).

Dada, A.O., Muradov, K.M., Davies, D.R.: Novel Solutions and Interpretation Methods for Transient, Sandface Temperature in Vertical, Dry Gas Producing Wells. *Proc. SPE Intelligent Energy International Conference and Exhibition 2016*, Aberdeen, United Kingdom. (2016).

Dada, A., Muradov, K., Dadzie, K., Davies, D.: Numerical and analytical modelling of sandface temperature in a dry gas producing well. *Journal of Natural Gas Science and Engineering 2017*. pp. 189-207.

Horner, D.R.: Pressure buildup in wells. Proc. Third World Petroleum Congress-Section II 1951, The Hague, Netherlands. (1951).

IAPWS, 1996. Release on the IAPWS formulation 1995 for the thermodynamic properties of ordinary water substances for general and scientific use. Int. Assoc. Prop. Water Steam (available from) ⟨http://www.iapws.org⟩.

IAPWS, 2008. Release on the IAPWS formulation 2008 for the viscosity of ordinary water substance. Int. Assoc. Prop. Water Steam. (available from) ⟨http://www.iapws.org⟩

Mclean, K., Zarrouk, S.: Pressure transient analysis of geothermal wells: A framework for numerical modelling. *Journal of Renewable Energy 2017*. pp. 737-746

Mao, Y., Zeidouni, M.: Analytical Solutions for Temperature Transient Analysis and Near Wellbore Damaged Zone Characterization. *Proc. the SPE Reservoir Characterization and Simulation Conference and Exhibition 2017*, Abu Dhabi, UAE. (2017).

Onur, M., Sarak, H., Tureyen, O.I., Cinar, M., Satman, A.: A new nonisothermal lumped-parameter model for low temperature, liquid dominated geothermal reservoirs and its applications. *Proc. Thirty-Third Workshop on Geothermal Reservoir Engineering Stanford University 2008*, California, USA. (2008).

Onur, M., Palabiyik, Y.: Nonlinear Parameter Estimation Based on History Matching of Temperature Measurements for Single-Phase Liquid-Water Geothermal Reservoirs. *Proc. World Geothermal Congress 2015*, Melbourne, Australia. (2015).

Onur, M., Palabiyik, Y., Tureyen, O.I., Cinar, M.: Transient temperature behavior and analysis of single-phase liquid-water geothermal reservoirs during drawdown and buildup tests: Part II. Interpretation and analysis methodology with applications. *Journal of Petroleum Science and Engineering 2016*. pp. 657-669.

O'Sullivan, M.J., Croucher, A.E., Anderson, E.B., Kikuchic, T., Nakagomed, O.: An Automated Well-Test Analysis System (AWTAS). *Journal of Geothermics*. pp. 3–25. (2005).

Palabiyik, Y., Onur, M., Tureyen, O.I., Cinar, M.: Transient temperature behavior and analysis of single-phase

liquid-water geothermal reservoirs during drawdown and buildup tests: Part I. Theory, new analytical and approximate solutions. *Journal of Petroleum Science and Engineering 2016*. pp. 637-656. (2016).

Panini, F., Onur, M.: Parameter Estimation from Sandface Drawdown Temperature Transient Data in the Presence of a Skin Zone Near the Wellbore. *Proc. the SPE Europec featured at 80th EAGE Conference and Exhibition 2018*, Copenhagen, Denmark. (2018).

Pruess, K. TOUGH2 User's Guide, Version 2, Earth Sciences Division, Lawrence Berkeley National Laboratory University of California, Berkeley, California (2012)

Ramazanov, A.Sh., Valiullin, R.A., Sadretdinov, A.A., Shako, V.V., Pimenov, V.P., Fedorov, V.N.: Thermal Modeling for Characterisation of Near Wellbore Zone and Zonal Allocation. *Proc. 2010 SPE Russian Oil & Gas Technical Conference and Exhibition 2010*, Moscow, Russia. (2010).

Ramey, H.J.: Wellbore Heat Transmission. *Journal of Petroleum Technology 1962*. pp. 427-435. (1962).

Sidorova, M., Shako, V., Pimenov, V., Theuveny, B.: The value of transient temperature responses in testing operations. *Proc. SPE Middle East Oil & Gas Show and Conference 2015*, Manama, Bahrain. (2015).

Silva Junior, M.F., Muradov, K., Carvalho, M.S.: Modeling and Analysis of Temperature Transients Caused by Step-Like Change of Downhole Flow Control Device Flow Area. *Proc. SPE Latin American and Caribbean Petroleum Engineering Conference 2012*, Mexico City, Mexico. (2012).

Somerton, W.H., 1992. Thermal Properties and Temperature-Related Behavior of Rock/Fluid Systems. Elsevier, New York, USA.

Zarrouk, S., O'Sullivan, M., Croucher, A., Mannington, W.: Numerical modelling of production from the Poihipi dry steam zone: wairakei geothermal system, New Zealand. *Journal of Geothermics 2007*. pp 289–303. (2007).

ISSN2703-4275